

# EFFECT OF WELL-DISPERSED NANO-TiO<sub>2</sub> ON SULPHOALUMINATE CEMENT HYDRATION AND ITS APPLICATION IN PHOTO-DEGRADATION

HAN WANG<sup>\*,\*\*</sup>, #PIQI ZHAO<sup>\*,\*\*</sup>, SHOUDE WANG<sup>\*,\*\*</sup>, LINGCHAO LU<sup>\*,\*\*</sup>, XIN CHENG<sup>\*,\*\*</sup>

<sup>\*</sup>Shandong Provincial Key Laboratory of Preparation and Measurement of Building Materials (University of Jinan),  
Shandong 250022, China

<sup>\*\*</sup>School of Material Science and Engineering, University of Jinan,  
Shandong 250022, China

<sup>#</sup>E-mail: 893000708@qq.com

Submitted March 21, 2017; accepted June 2, 2017

**Keywords:** Nano-TiO<sub>2</sub>, Sulphoaluminate cement, Hydration, Photo-degradation

*Nano-TiO<sub>2</sub> and sulphoaluminate cement have been received sustained attention due to their environment-friendly characteristic, respectively. Particular attention was paid to their materials composite. To better understand the effect of nano-TiO<sub>2</sub> on sulphoaluminate cement hydration and its application in photo-degradation, the composite systems of cement paste (mortar) with well-dispersed nano-TiO<sub>2</sub> were investigated by mechanical analysis, Rietveld/XRD, SEM, porosity analysis and photocatalytic test. The results reveal that nano-TiO<sub>2</sub> can be well dispersed under ultrasonic treatment of 15 min when the sodium hexametaphosphat is chosen as the dispersant. And the well-dispersed nano-TiO<sub>2</sub>, with the dosage of 0.2 wt. %, has the most significant effect on the mechanical improvement. Micro-analysis show that the mechanical promotion by nano-TiO<sub>2</sub> is not attributed to the hydration degree increase but microstructure optimization. It is reflected in the decrease of porosity, mainly affecting the transitional pores ( $D = 10 \sim 100$  nm), and spatial structures modification of cement paste where AFt was more likely to form as needle shape with shorter length-diameter ratio. The photocatalytic test demonstrates that the composite system (cement paste) has long-term effective photo-degradation property.*

## INTRODUCTION

Recently, photocatalysis has developed rapidly, which has been widely used in the fields of anti-microbial, sewage treatment, water electrolysis, air purification and anti-corrosion [1-3]. As the representative of green technology, photocatalysis is attracted by academia and commerce. Nano-TiO<sub>2</sub> (NT), due to its inherent advantages of high catalytic efficiency, good thermal stability, low cost and environmental protection, has become the best received photocatalysis material [4-5]. Furthermore, anatase-TiO<sub>2</sub> as one of the crystal forms demonstrated more outstanding performance. Its structure unit of titanium-oxygen octahedron with a lot crystal lattice disfigurement is more beneficial to separate photoelectrons from vacancies and the wider band gap (anatase-TiO<sub>2</sub>: 3.2 eV, rutile-TiO<sub>2</sub>: 3.0 eV) can prevent recombination of electrons and holes. In addition, its surface easily adsorbed the necessary materials as H<sub>2</sub>O, O<sub>2</sub> [6]. However, the disadvantages of easy-to-lost based on the matrix limit its application. At present, the effective way to solve this problem is to load the NT on inorganic materials such as glass, cement and ceramic [7-10]. The cement-based materials have special porous structure characteristics, which can enhance the capacity of absorbing pollutants and then can improve the efficiency of

photocatalysis [11]. Some studies also explored that the NT is also beneficial to cementitious matrix. It can improve and modify the mechanical performance, and regulate and control the growth of hydration products [12]. Bo reported that hydration products were formed on greater surface areas and the early rate of hydration can be altered by chemically nonreactive NT particles [13]. Ma has addressed that NT could decrease the hydration induction period of cement paste and make the hydration acceleration period in advance, but has no influence on the deceleration and stabilization periods [14].

Although some progress about the composite system have been made, agglomeration of NT was the main obstacles in the study of NT on the hydration of cement-based materials. Thus, academia focused their attention on the difficulty. Dry mix, solvent dispersion included ultrasonic, mechanical stirring, treatment with dispersant were adopted in the research. Folli A dry mixed NT and white Portland cement (52.5, w/c = 0.4) powders in the mass ratio 3.5 : 96.5, and certified paste samples containing NT have the ability of discolouring Rhodamine B under UV light [15]. Feng D had the NT particles soaked in water and ultrasonically vibrated for 30 min to achieve good distribution [16]. B G. Ma added NT to deionized water, which was stirred and dispersed by ultrasonication at 325 W for 30 min to

obtain the uniform suspensions. Than the influence of NT on physical and hydration characteristics of fly ash-cement systems was researched [14]. Allahverdi A. found that the proper mixing design and dispersion of NT in saturated lime water by ultrasound, not only led to proper distribution of NT in cement, but also increased the photocatalytic properties of system under UV radiation and visible light [17]. However, little is involved in characteristics for dispersion degree and the effect of the dispersion system of NT on the hydration and photo-degradation of cement-based materials.

Nowadays, the types of cement can be generally divided as Portland cement, aluminate cement and SAC. The SAC is the representative of "GREEN" cement due to its higher waste utilization, lower energy requirement and lesser air-pollution emissions. And the CO<sub>2</sub> emission were decreased by nearly 40 % than that of Portland cement. Moreover, SAC has such inherent advantages as high early strength, short setting time, low shrinkage and expansion. It also demonstrated good performance of low alkalinity, good durability [18-20]. In this article, sulfoaluminate cement was been investigated as a powerful materials to reduce the pressure on resources and environment.

The aim of this work was to know the hydration of SAC was influenced by well-dispersed NT suspensions, and its application in photo-degradation. The ultimate objective is to lay the foundation for follow-up research about the application of NT in sulfoaluminate cement-based materials.

## EXPERIMENTAL

### Materials

The SAC (42.5-grade, China United Cement Corporation, China) was selected as primary material, which accords with the requirements of GB20472-2006 [21]. NT (Aladdin-Holding Group, China) used was 40 nm in length and anatase structure in crystal composition. Chemical composition of SAC and NT was determined by XRF (SRS3400, Bruker AXS Corporation, Germany) and summarized in Table 1.

Table 1. Chemical composition of SAC and NT (wt. %).

	SAC	NT
CaO	46.6	—
Al <sub>2</sub> O <sub>3</sub>	20.5	—
SO <sub>3</sub>	12.3	—
SiO <sub>2</sub>	8.8	—
Fe <sub>2</sub> O <sub>3</sub>	2.0	—
MgO	1.4	—
Others	8.4	—
TiO <sub>2</sub>		>99.5

### Specimen preparation

Suspensions (6 g·l<sup>-1</sup>) were prepared by dissolving NT in deionized water (DI-water). Then the suspensions was treated separately as follow, mechanical dispersion, dispersion by dispersant, ultrasonic dispersion and their combination. Magnetic stirrers apparatus, with a high speed of 1600 rpm was used for mechanical stirring. KQ-400KDE high power ultrasonic cleaning, with the power of 100 W, was used for ultrasonic dispersion. Polycarboxylate superplasticizer (PCS, the solid content is 42.91 %, Jiangsu Sobute, China) and sodium hexametaphosphat (SH, Sinopharm Chemical Reagent Co. Ltd, China) was selected as dispersant, respectively. Moreover, their dosage took 4 % of the NT dosage in this research.

The above suspension treatments are detailed in Table 2. Specimen of A~E are obtained by different dispersion methods, respectively. Also, the whole process was strictly maintained in water bath at 20°C to avoid the effect of temperature on the dispersion result.

Table 2. Various dispersion methods.

	stirring	ultrasonic	Dispersant PCS	SH
A	○ <sup>a</sup>	× <sup>b</sup>	×	×
B	○	×	○	×
C	×	○	×	×
D	×	○	○	×
E	×	○	×	○

<sup>a</sup> Taking the dispersion methods, <sup>b</sup> Not taking the dispersion methods

Table 3. Mix proportions of mortars and pastes.

NT dosage (%)	Specimens	Mixture components (g)			
		NT	SAC	Water	Sand
<i>Pastes</i>					
0	P0	0	500	135	–
0	PH	0	500	135	–
0.02	PZ2	0.1	500	135	–
0.05	PZ5	0.25	500	135	–
0.1	P1	0.5	500	135	–
0.2	P2	1	500	135	–
0.3	P3	1.5	500	135	–
<i>Mortars</i>					
0	M0	0	450	225	1350
0.02	MZ2	0.1	450	225	1350
0.05	MZ5	0.23	450	225	1350
0.1	M1	0.45	450	225	1350
0.2	M2	0.9	450	225	1350
0.3	M3	1.35	450	225	1350

With the appropriate amount of NT (from 0 to 0.3 % by mass of cement) were added to the DI-water by the the above optimal dispersion method before cement

pastes and mortars were cast. Moreover, to verify the influence of SH on the SAC hydration, the biggest dosage SH (0.06 g) was added to the DI-water as contrast experiment and named "PH". The mix proportions of the pastes and mortars are listed in Table 3. The SAC pastes and mortars were prepared with the water to cement (W/C) weight ratio of 0.27 and 0.5, respectively. The mortar specimens were prepared according to GB/T 17671-1999 [22] and cement to standard sand weight ratio of 1/3. After compacted by vibration, the specimens were cured in standard curing box ( $21 \pm 2^\circ\text{C}$ /90 % RH) for 1d, 3d, 7d, 28d. At stipulated age, specified samples were taken out and tested.

#### Data collection and processing

The setting times and fluidity of SAC pastes were measured in accordance with GB/T 1346-2001 by a manual Vicat apparatus [23], and the compressive strength were carried out at a loading speed of  $2.5 \text{ kN}\cdot\text{s}^{-1}$ . The mechanical strength of mortars were tested by GB/T 17671-1999.

X-ray powder diffraction patterns (XRD) were recorded in Bragg-Brentano reflection geometry ( $\theta/2\theta$ ) on the Bruker X-ray diffractometer (D8-Advance, Bruker International Corporation, German) and the patterns were refined by the Rietveld method with TOPAS software. The porosity and pore size distribution of hardened SAC pastes were measured by mercury injection apparatus (MIP Micromeritics, AutoProe 9500 IV). The morphology of the SAC pastes was being presented in SEM images by scanning electron microscope (Quanta FEG 250 field emission scanning electron microscope, America).

The photocatalytic performance of TiO<sub>2</sub>-cement system was evaluated by the degradation of methyl orange (MO, Aladdin-Holding Group, China,  $10 \text{ mg}\cdot\text{l}^{-1}$ , 30 ml) dye under UV light irradiation. Prior to the photocatalytic test, 5 g ground cement pastes was placed in the configured dye solution and the solution was magnetically stirred in the dark for 60 min. In the test, every 2 ml of the solution was collected and measured the absorbance values at irradiation time interval of 1 h.

Light absorption method was used to determine the concentration of suspensions in order to assess the dispersion degree and photo-degradation rate. Spectrophotometer (A UV-5200 PC, Shanghai Metash Instruments Co. Ltd, China) was used in the test. The absorbance values is direct proportional to the concentration of suspensions and its standard formula is

$$A = a \cdot l \cdot c \quad (1)$$

( $a$  is the nature of the material as absorption coefficient,  $l$  is a distance light through the media,  $c$  is concentration of suspensions).

## RESULTS AND DISCUSSIONS

### NT dispersion in DI-water

Figure 1 depicted the absorbance curves of NT suspensions varied with the treating times. The curve reveals that absorbance rises at the beginning and then declines with increasing treating time. For all dispersion methods, 15 min as the optimal treating time is determined as the maximum of the curves. Initially, NT based on the energy from the ultrasonic or shear force significantly reduce the agglomeration of the nano-particles. After 15 min, excess energy is being in the NT suspensions and the nano-particles tend to be re-agglomerated.

Compared A, B, the effect of ultrasonic dispersion for C, D and E is obviously superior to mechanical dispersion. Ultrasonic can raise the volume and energy utilization. The C, D and E curves revealed dispersant was added to increase the heat of wetting and improve the dispersing effect on the basis of ultrasonic dispersion and mechanical dispersion, and SH is better than PCS. According to analyses above, it is suggested that and SH as dispersant and 15 min ultrasonic treatment was preferred when using DI-water as dispersion medium.

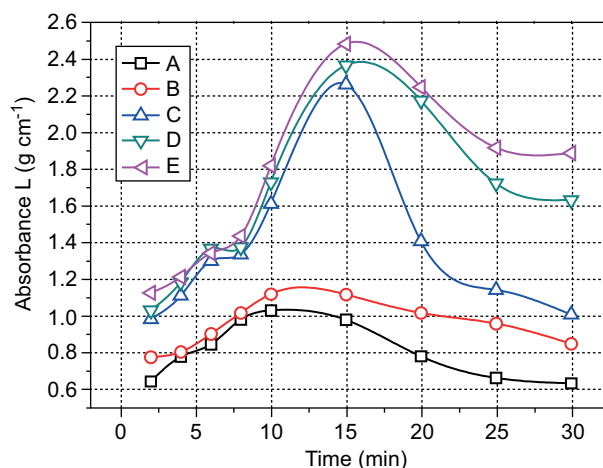


Figure 1. The effect of various dispersion methods on the absorbance.

### Compressive strength of cement pastes

The effect of NT on compressive strength of the SAC pastes are graphically represented in Figure 2. At the early hydration ages, the rapid hardening characteristic of SAC leads to a significant increase in the compressive strength. Meanwhile, it slightly increases for all specimens during the hydration proceed. Figure 2 also reveals that different dosages of NT have correspondingly positive effect on the compressive strength development. Compared with each certain hydration ages, it basically increases first and then decreases at the added dosages of NT. The specimen of P2, adding 0.2 % of NT, showed best performance. It reached 141.6 Mpa, 1.7 times higher than the blank, when curing at 28d. The positive effect

of NT on the compressive strength of cement paste was also reported in elsewhere [13, 24], which was explained as its role of crystallization-induction and pore structure-modification. However, when  $\text{TiO}_2$  Dosage is the same, the strength development of the SAC pastes is enormously boosted and superior to the past research. This responds well-dispersed NT have the more effective impacts on the hydration of SAC. And the further explanation were taken by the following micro-analysis. Compared with P0, the compressive of PH show a little decrease about 1.5 Mpa in the early age(1d, 3d), however, 0.7 Mpa and 0.4 Mpa in the later age (7d, 28d), which illustrates the influence of SH on the SAC retarded slightly, negligible, thus, the effect of SH is nearly negligible.

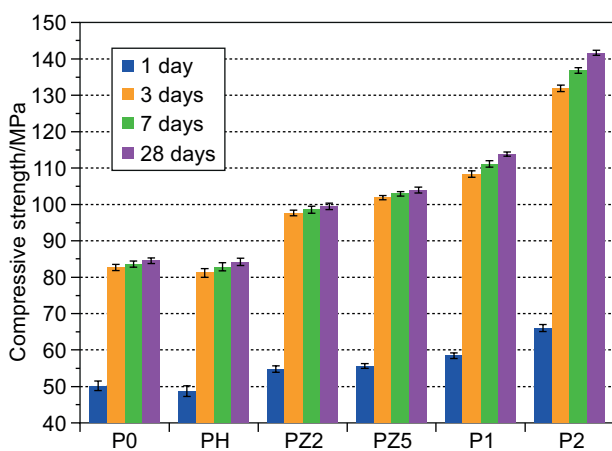


Figure 2. Effect of NT on the compressive strength of SAC pastes.

#### Mechanical strength of mortar

The NT was further added in the SAC-mortar system with the corresponding NT-cement ratios from 0.1 % to 0.3 %. The compressive and flexure strength are reported in Figure 3 and Figure 4, respectively. There are also some beneficial effect on both compressive and flexure strength of mortar contributed by NT. The enhancement has become more significant when the dosage of NT is larger than 0.05 %, especially in the later hydration period. It is indicated that only if the dosage of NT satisfies a certain quantity ( $> 0.05\%$ ), can its effect on cement hydration acceleration and structure improvement obviously appear in mortar system. The reason why it seems less sensitive than SAC paste based on the contribution to mechanical strength by NT is mainly because the ratio of matrix-defect improvement in mortar system is less than pastes at certain hydration age. In this work, both M2 (0.2 % dosage) and M3 (0.3 % dosage) showed the satisfactory mechanical performance and M3 was reported to have the better flexural strength. Compared with the neat specimens, the compressive and flexural strength of M3 were respectively increased by 13.06 %, 35.12 % at 1d, 26.95 %, 36.02 % at 3d, 40.28 %, 37.33 % at 7d and 39.45 %, 38.19 % at 28d.

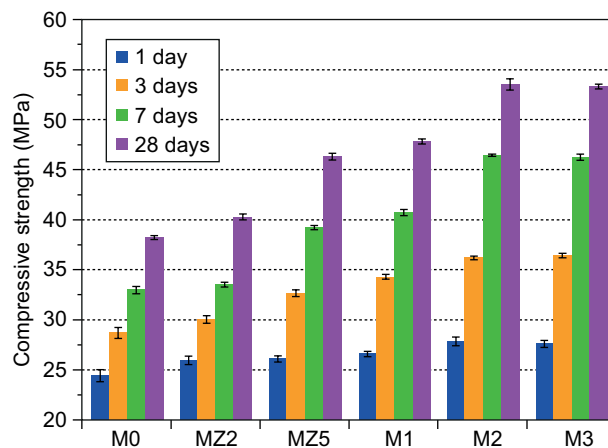


Figure 3. Effects of NT on the compressive strength of cement mortar (W/C = 0.5).

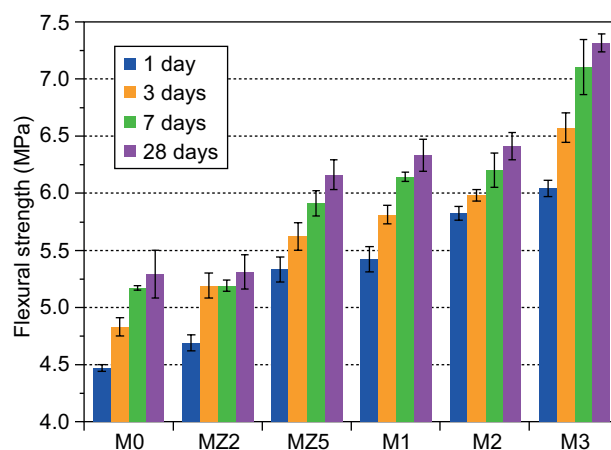


Figure 4. Effects of NT on the flexural strength of cement mortar (W/C = 0.5).

#### Rietveld quantitative phase analysis of cement pastes

To evaluate the effect of NT on the composition of hydration products, the Rietveld quantitative phase analysis of P0 and P2 specimens were compared supporting by the TOPAS software. In the initial refinement cycles, the global parameters, i.e. zero error, air scattering factor, and phase scale factors, were refined. The background was fitted by Chebychev function with 5 or 6 terms of polynomial equation. Cell parameters, absorption factor and crystalline size and strain of the main crystal phases were carefully refined within constrained limits when necessary. The refinement was carried out by several cycles until the stable R factor and satisfactory fits were obtained. The final Rietveld plot (3d) is reported in Figure 6 and quantitative results (1d, 3d, 7d and 28d) are provided in Table 4.

From the results of Rietveld quantitative phase analysis, most absolute deviations of unhydrated minerals and hydration products at specific hydration age are less



than 2 %, which means the content of hydration products is not obviously increased and the hydration degree tends towards consistent when well-dispersed NT was added. The results reveal the mechanical improvement of SAC pastes and mortars is not attributed to the increase of hydration degree but other reasons.

#### Porosity and pore size distribution

To check whether the NT plays a role in structure modification of SAC paste, the porosity and pore size distribution analysis were implemented. The results of P0 and P2 samples at 3d of hydration time were compared and depicted in Figure 6. The total porosity of P2 sample

Table 4. Rietveld quantitative phase analysis of SAC pastes at 3d.

Analysis	Phases and R-factors	Rietveld (wt. %)							
		1 d		3 d		7 d		28 d	
		P0	P2	P0	P2	P0	P2	P0	P2
Quantitative results	AFt	21.37	24.37	30.80	31.65	30.11	32.28	32.90	34.40
	C <sub>4</sub> A <sub>3</sub> \$	17.97	17.17	10.94	9.56	10.12	8.19	9.08	7.56
	β-C <sub>2</sub> S	16.18	18.46	14.97	14.83	15.03	14.23	13.56	14.01
	CaCO <sub>3</sub>	14.06	12.28	12.68	12.67	12.81	12.63	12.92	12.11
	CaSO <sub>4</sub>	3.53	2.60	2.67	2.67	2.69	2.66	2.72	2.55
	C <sub>3</sub> A	7.29	6.28	6.95	6.95	7.02	6.93	7.08	6.64
	C <sub>12</sub> A <sub>7</sub>	0.85	1.35	—	—	—	—	—	—
	α-C <sub>2</sub> S	3.38	3.01	3.65	4.01	3.24	3.51	3.82	4.12
	C <sub>4</sub> AF	5.01	4.67	3.68	3.62	3.95	3.64	3.39	3.62
	CaMg(CO <sub>3</sub> ) <sub>2</sub>	5.71	4.70	4.86	4.81	5.76	5.99	5.26	5.20
	AH <sub>3</sub>	4.64	5.11	8.79	9.22	9.26	9.97	9.27	9.78
Criteria of fit	RWP	6.27	6.82	6.87	7.31	7.25	7.29	7.16	7.15
	RP	4.80	5.20	5.29	5.61	5.53	5.45	5.42	5.29

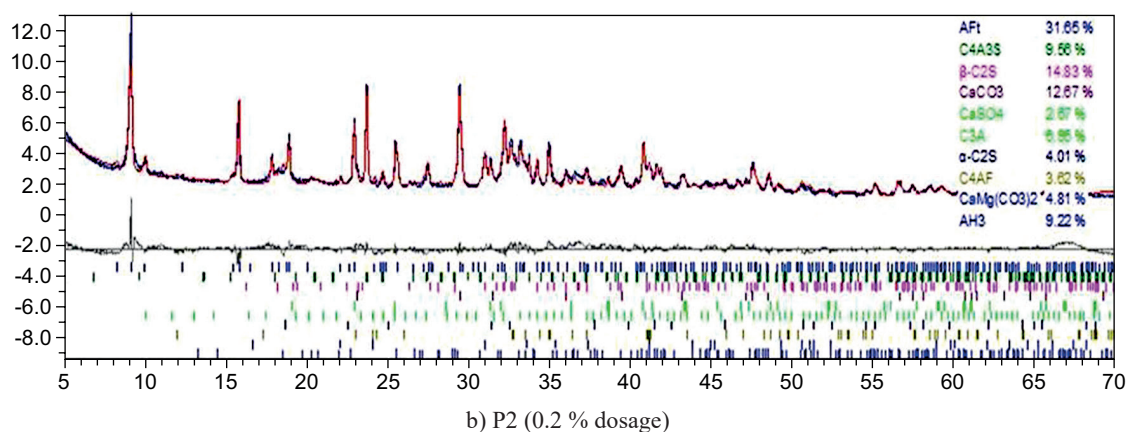
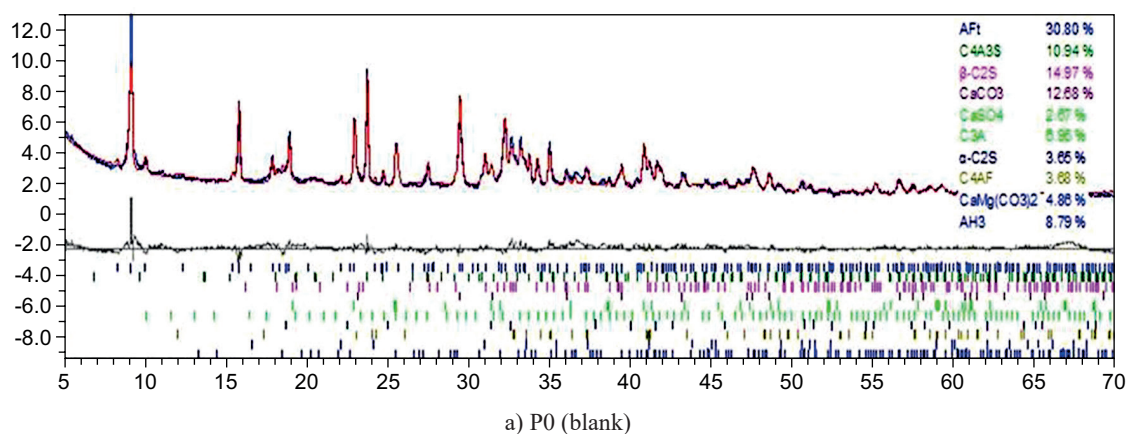


Figure 5. Rietveld quantitative XRD pattern of SAC pastes at 3 d: a) P0 (blank), b) P2 (0.2 % dosage).

is  $8.2 \text{ ml}\cdot\text{g}^{-1}$ , about 2.7 % lower than the blank sample (P0), which revealed the NT particles has significant effect on decreasing porosity of SAC paste. In addition, from the analysis of pore size distribution, the NT particle mainly contribute to nano-size pore modification. When the pore size is less than 10 nm or more than 100 nm, two specimens were mostly same. The major difference is that NT modified the pore diameter from 10 nm to 100 nm. The conglomerations containing the nano-particles as nucleus expanded and filled up the pore space around them gradually. The hydration products accumulated

rapidly and grew outwards into the water filled voids, so porosity was decreased. Moreover, it should be noticed that the reduction of porosity mainly occurred within the capillary pore range. Capillary pores are considered remnants of the water-filled space between the hydrated cement grains [25]. It is possible that hydration medium environment was greatly stimulated by a small quantity of NT particles.

### SEM analysis

The SEM images of P0 and P2 specimens at 3d of hydration time are shown in Figure 7. It is shown that the P2 specimens (Figure 7a) has a more uniform and denser paste structure than P0 (Figure 7d), which is corresponded to the porosity and pore structure distribution analysis above. And the needle bar Aft phase in P2, due to the super surfactivity of nano-particles, incline to form with shorter length-diameter ratio compared with P0. For SAC, the needle bar structure is disadvantageous due to its inhomogeneity highly as the Figure 7f shows. This structure can influence the quality of hardened paste, even causes the strength reduction for latter period [26]. Furthermore, AFt and AFm grew staggered in P2, incline to establish a three-dimensional network structure which is directly related to the hardening of SAC pastes. Moreover, Ekincioglu and Ozkul confirmed NT addition can be a solution for reducing water sensitivity of sulpoaluminate cement, titanate coupling

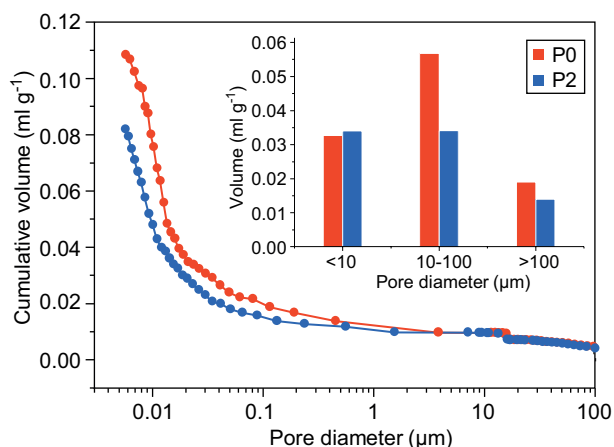


Figure 6. Porosity and pore size distribution of SAC paste at 3 d.

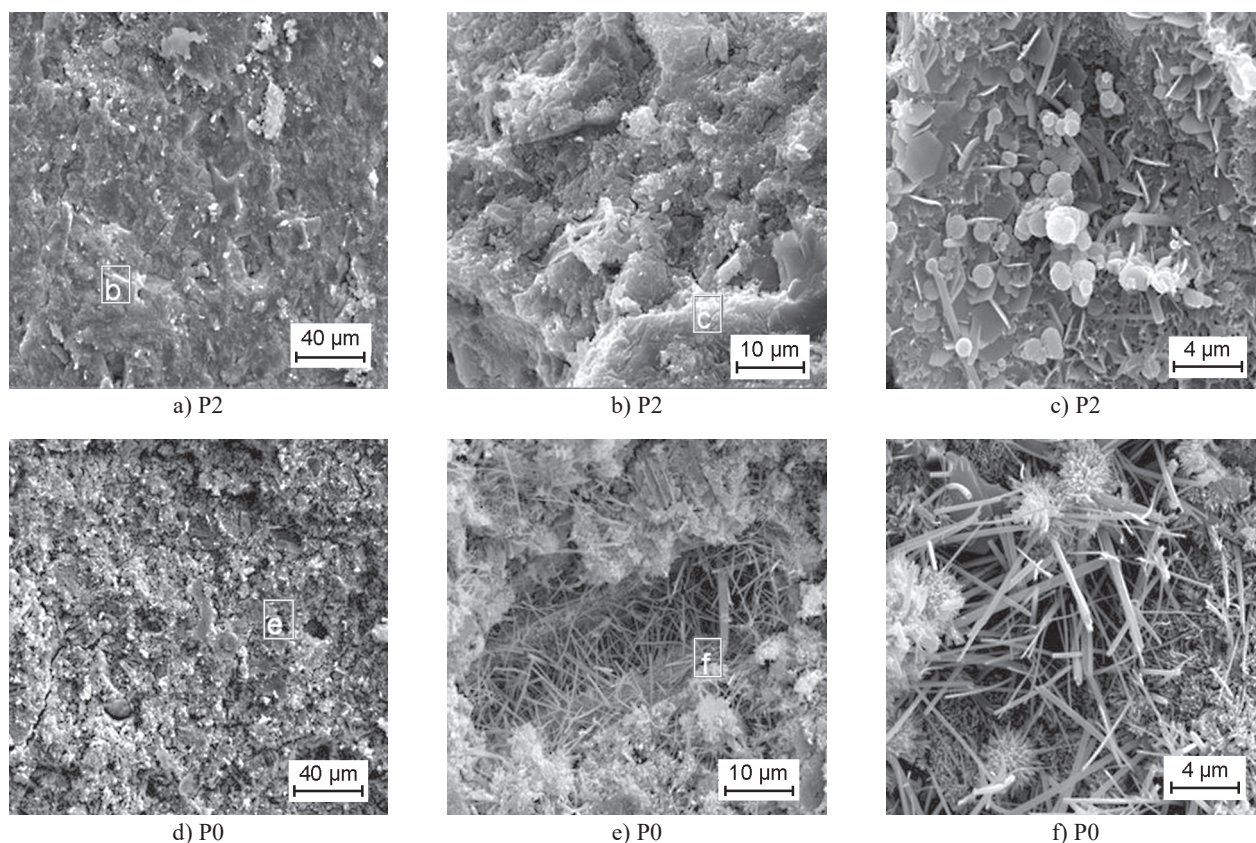


Figure 7. The SEM image of SAC pastes (a, b and c is P2, d, e and f is P0).

agents improve the moisture sensitivity of composite materials. Eventually, the Me–O–Ti–O–Me (Me is cement hydrates) bond make cement hydrates form a more stable network [27–29], as is shown in Figure 7b. These microstructure analysis results validating fully that the strength promotion of SAC pastes is related to the above compressive strength result.

#### Photo-degradation test

The well-dispersed NT modified dramatically the hydration process of SAC, than the photo-degradation ability of the composite system was investigated.

The result of degradation of MO dye is shown in Figure 8, and Figure 8a and b represent the specimens of SAC pastes at 3d and 28d. In the Figure 8a, three curves have decreased to varying degrees with time. This illustrates the MO dye can be self-degraded under UV radiation and can be absorbed on the SAC pastes. The decline of specimens with NT is the most apparent,

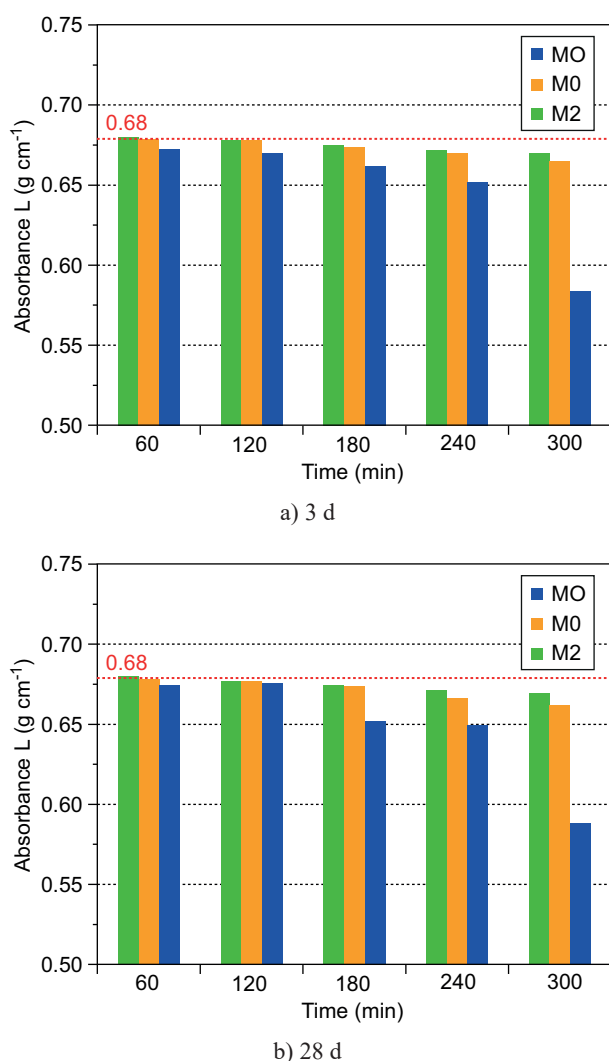


Figure 8. Photo-degradation of MO, M0 and M2 at: a) 3 d; b) 28 d.

the absorbance of MO declined from 0.68 to 0.53 at 300 min. As the existence of pores in cement, which increase the contact between O<sub>2</sub>/H<sub>2</sub>O and NT in cement-based materials. O<sub>2</sub>/H<sub>2</sub>O is the requirement of photocatalytic activity. The results depicted that the photo-degradation of SAC pastes was effective. Due to the bonding of NT and load was reinforced, Figure 8b showed the homogeneous trend and the system still possessed the photo-degradation ability. The result proved that the well-dispersed NT in cement can deliver photo-degradation performance.

#### CONCLUSION

Combined with SAC as the matrix, the well-dispersed NT can not only significantly improve the mechanical properties but also make it have long-term photo-degradation characteristic. Detailed conclusions are listed as follows.

- Ultrasonic treatment time (100W of the output power) of 15 min with SH as dispersant are preferred for obtaining well-dispersed NT.
- The dosage of NT about 0.2 wt. %, compared with SAC, is the optimum proportion. And the compressive strength is promoted by 31.8 % at 3d and 67.5 % at 28d, respectively. The mortar with dosage of NT about 0.3 wt. % shows the best mechanical strength with increase of 27.4 % (3d) and 40.3 % (28d) in compressive strength and 36.0 % (3d) and 38.2 % (28d) in flexural strength. The above mechanical promotions by NT are not attributed to the hydration degree increase but microstructure optimization.
- The NT particles mainly contribute to transitional pores (D = 10 ~ 100 nm) modification and the total porosity of SAC paste (P2) decreased by 2.7 % compared with the blank sample (P0). Spatial structures improvement is another reason leading to better mechanical property. The AFt phase in SAC paste, influenced by NT particles, inclines to form shorter length-diameter ratio needle-shape. And it is grown intermingled with sheet-like AFm and amorphous gel, forming the dense microstructure.
- The composite system of SAC and NT have long-term effective photo-degradation property, which is hopeful to prepare the SAC cement-based coating materials applied in environmental treatment.

#### Acknowledgements

This work was supported by the project of National Natural Science Foundation of China (No.51602126). We also thank the Program for Scientific Research Innovation Team in the Colleges and Universities of Shandong Province.



## REFERENCE

- Chen X., Mao S. S. (2007): Titanium Dioxide Nanomaterials: Synthesis, Properties, Modifications, and Applications. *Chemical Reviews*, 107, 2891-2959. doi:10.1021/cr0500535
- Tong H., Ouyang S., Bi Y., Umezawa N., Oshikiri M., Ye J. H. (2012): Nano-photocatalytic Materials: Possibilities and Challenges. *Advanced Materials*, 24, 229-251. doi:10.1002/adma.201102752
- Herrmann J. M., Duchamp C., Karkmaz M., Hoai BT., Lachheb H., Puzenat E., Guillard C. (2007): Environmental green chemistry as defined by photocatalysis. *Journal of Hazardous Materials*, 146, 624-629. doi:10.1016/j.jhazmat.2007.04.095
- Yang H. G., Sun C. H., Qiao S. Z., Zou J., Liu G., Smith S. C., Cheng H. M., Lu G. Q. (2008): Anatase TiO<sub>2</sub> single crystals with a large percentage of reactive facets. *Nature*, 453, 638-641. doi: 10.1038/nature06964
- Xing Z., Zhou W., Du F., Qu Y., Tian G., Pan K., Tian C., Fu H. (2014): A floating macro/mesoporous crystalline anatase TiO<sub>2</sub> ceramic with enhanced photocatalytic performance for recalcitrant wastewater degradation. *Dalton Transactions*, 43, 790-798. doi:10.1039/c3dt52433g
- Nakata K., Fujishima A. (2012): TiO<sub>2</sub> photocatalysis: Design and applications. *Journal of Photochemistry & Photobiology C Photochemistry Reviews*, 13, 169-189. doi:10.1016/j.jphotochemrev.2012.06.001
- Chang H. K., Kim B. H., Yang K. S. (2012): TiO<sub>2</sub> nanoparticles loaded on graphene/carbon composite nanofibers by electrospinning for increased photocatalysis. *Carbon*, 50, 2472-2481. doi:10.1016/j.carbon.2012.01.069
- Ollis D., Pichat P., Serpone N. (2010): TiO<sub>2</sub> photocatalysis-25 years Preface. *Applied Catalysis B Environmental*, 99, 377-377. doi: 10.1016/j.apcatb.2010.06.030
- Lewis J. A., Boyer M., Bentz D. P. (1994): Binder Distribution in Macro-Defect-Free Cements: Relation between Percolative Properties and Moisture Absorption Kinetics. *Journal of the American Ceramic Society*, 77(3), 711-716. doi:10.1111/j.1151-2916.1994.tb05429.x
- Drabik M. (2009): Cheminform abstract: contribution of materials chemistry to the knowledge of macro-defect-free (mdf) materials. *Pure & Applied Chemistry*, 41, 1413-1421. doi:10.1351/PAC-CON-08-07-16
- Yazawa T., Machida F., Oki K., Mineshige A., Kobune M. (2009): Novel porous TiO<sub>2</sub>, glass-ceramics with highly photocatalytic ability. *Ceramics International*, 35, 1693-1697. doi:10.1016/j.ceramint.2008.09.011
- Chen L., Yang S., Mader E., Ma P.C. (2014): Controlled synthesis of hierarchical TiO<sub>2</sub> nanoparticles on glass fibres and their photocatalytic performance. *Dalton Transactions*, 43, 12743-53. doi:10.1039/c4dt00977k
- Bo Y. L., Jayapalan A. R., Kurtis K. E. (2013): Effects of nano-TiO<sub>2</sub> on properties of cement-based materials. *Magazine of Concrete Research*, 65, 1293-1302. doi:10.1680/macr.13.00131
- Ma B. G., Li H. N., Li X. G., Mei J. P., Lv Y. (2016): Influence of nano-TiO<sub>2</sub> on physical and hydration characteristics of fly ash-cement systems. *Construction and Building Materials*, 122, 242-253. doi: 10.1016/j.conbuildmat.2016.02.087
- Folli A., Pochard I., Nonat A., Jakobsen U. H., Shepherd A. M., Macphee D. E. (2010): Engineering photocatalytic cements: understanding TiO<sub>2</sub> surface chemistry to control and modulate photocatalytic performances. *Journal of the American Ceramic Society*, 93, 3360-3369. doi: 10.1111/j.1551-2916.2010.03838.x
- Feng D., Ning X., Gong C., Zhen L., Xiao H., Hui L. (2013): Portland cement paste modified by TiO<sub>2</sub> nanoparticles: a microstructure perspective. *Industrial & Engineering Chemistry Research*, 52, 11575-11582. doi: 10.1021/ie4011595
- Allahverdi A., Yousefi A., Hejazi P. (2013): Effective dispersion of nano-TiO<sub>2</sub> powder for enhancement of photocatalytic properties in cement mixes. *Construction and Building Materials*, 41, 224-230. doi: 10.1016/j.conbuildmat.2012.11.057
- Zhou H., Liu J., Liu J., Li C. (2012): Hydration kinetics process of low alkalinity sulfoaluminate cement and its thermodynamical properties. *Procedia Engineering*, 27, 323-331. doi:10.1016/j.proeng.2011.12.459
- Kuryatnyk T., Chabannet M., Ambroise J., Pera J. (2010): Leaching behaviour of mixtures containing plaster of Paris and calcium sulfoaluminate clinker. *Cement and Concrete Research*, 40, 1149-1156. doi:10.1016/j.cemconres.2010.03.013
- Quillin K. (2001): Performance of belite-sulfoaluminate cements. *Cement and Concrete Research*, 31, 1341-1349. doi: 10.1016/S0008-8846(01)00543-9.
- GB/T 17671 CNS, Method of testing cements-Determination of strength, 1999.
- GB/T 20472 CNS, Sulphoaluminate Cement, 2006.
- GB/T 1346 CNS, Test methods for water requirement of normal consistency, setting time and soundness of the Portland cements, 2001.
- Khataee R., Heydari V., Moradkhannejhad L., Safarpour M., Joo S.W. (2013): Self-cleaning and mechanical properties of modified white cement with nanostructured TiO<sub>2</sub>. *Journal of Nanoscience & Nanotechnology*, 13, 5109-5114. doi:10.1166/jnn.2013.7586
- Chen J., Kou S. C., Poon C. S. (2012): Hydration and properties of nano-TiO<sub>2</sub>, blended cement composites. *Cement and Concrete Composites*, 34, 642-649. doi:10.1016/j.cemconcomp.2012.02.009
- Glasser F. P., Zhang L. (2001): High-performance cement matrices based on calcium sulfoaluminate-belite compositions. *Cement and Concrete Research*, 31, 1881-1886. doi:10.1016/S0008-8846(01)00649-4
- Ekincioglu O., Ozkul M. H., Struble L. J., Patachia S. (2012): Optimization of material characteristics of macro-defect free cement. *Cement and Concrete Composites*, 34, 556-565. doi:10.1016/j.cemconcomp.2011.11.003
- Ekincioglu O., Ozkul M. H., Patachia S., Moise G. (2013): Effect of TiO<sub>2</sub> addition on the properties of macro defect free cement-polymer composites. *Restoration of Buildings & Monuments*, 19, 125-134. doi:10.1515/rbm-2013-6587
- Drabik M., Galikova L., Billik P., Maier G., Kosednar Legenstein B. (2013): Macro defect free materials; mechanochemical activation of raw mixes as the intensifying tool of the entire mdf synthesis. *Ceramics-Silikáty*, 57, 120-125.